

Network Analysis of the State Space of Discrete Dynamical Systems

Amer Shreim,¹ Peter Grassberger,¹ Walter Nadler,² Björn Samuelsson,³ Joshua E.S. Socolar,³ and Maya Paczuski¹

¹*Complexity Science Group, Department of Physics and Astronomy,
University of Calgary, Calgary, Alberta, Canada*

²*Department of Physics, Michigan Technological University, Houghton, Michigan, USA*

³*Department of Physics, Duke University, Durham, North Carolina, USA*

(Dated: October 27, 2019)

We study networks generated by the dynamics of elementary 1-d cellular automata (CA) on finite lattices. Many such CA make simple networks, whereas others form statistically heterogeneous and sometimes scale-free networks. Analytic results are obtained for the scaling of the hubs with system size for a variety of CA including rules 22, 54, 110. For rule 4 also the asymptotic in-degree distribution is obtained. We further define the *path diversity* of the network, which may also exhibit scaling behavior. Statistical heterogeneity of the state space network is discussed in the context of previous claims for classifying the complexity of dynamical systems by Wolfram and others. Our results quantify how complex state space networks arise from simple deterministic dynamics.

PACS numbers: 05.45.-a, 89.75.-k, 89.75.Fb, 89.75.Da

As physical theories widen into the biological or social realms, the problem of describing complex dynamical systems becomes increasingly important. Even elementary systems, such as cellular automata (CA) (originally proposed by von Neumann [1]) often exhibit dynamical patterns that are difficult to describe or characterize meaningfully. One approach has been to classify their behavior based on various definitions of complexity. These have largely focused on patterns generated in space and time. Despite a large body of work (see e.g. Ref. [2, 3, 4, 5, 6, 7]), such classification schemes have not in our view led to widely accepted applications, and other ways to characterize complex behaviour seem to be called for.

Here we take an alternative approach by describing dynamical systems using quantitative statistical measures for their state space network. For deterministic, discrete, dynamical systems the state space forms a directed network where each state is represented as a node and each node points to its dynamical successor [8]. For irreversible systems each state can have many “preimage” states. Using the terminology of networks, each node has out-degree one, while its in-degree may vary. The fact that network theory has recently led to progress in understanding physical [9], biological [10], technological [11] and social [12] phenomena, has prompted us to study dynamical systems from this viewpoint.

A variety of statistical measures have been used to characterize complex networks – e.g. their degree distribution, clustering coefficients and average path length [13, 14]. Many networks possess unexpected properties markedly different from random graphs, e.g. “fat-tailed” (the appearance of large hubs) and scale-free degree distribution. Such networks have e.g. been found empirically for regulatory networks [15], the world-wide web [11], and earthquakes [9]. These properties could reflect non-trivial organization caused by evolutionary dynamics, could be due to combinatorial constraints [16], or could have other reasons – as discussed in this work.

We find that a number of discrete, deterministic dynamical systems, which had been labeled as “complex” by various authors, exhibit highly heterogeneous network structure. Network heterogeneity includes: (1) local heterogeneity as measured by the in-degree distribution and (2) global heterogeneity as measured by a new quantity – the *path diversity* – which is defined later in the text. In several cases, the in-degree of the largest hub and path diversity scale with system size. Certain CA such as rules 22, 54, and 110 (in Wolfram’s notation [17]) exhibit scaling behavior for both measures – or, in other words, show strong fluctuations both locally (at the node level) and globally (at the path level). We speculate that network heterogeneity at multiple levels may be a generic property of the state space of dynamical systems exhibiting emergence, i.e. organized collective behavior that is not simple to describe.

As a test bed, we study several 1-d binary CA with nearest neighbor interactions. The state of a site i at time t depends on the values of the sites $i-1, i, i+1$ at the previous time $t-1$. Wolfram put these CA into four complexity classes [17, 18]. His classification was based on the qualitative appearance of spatio-temporal patterns produced from random initial conditions on large lattices. The four classes are: (I) The evolution almost always leads quickly to a unique fixed point. (II) It almost always leads quickly to one of many attractors with a small period. (III) The system doesn’t settle quickly into a periodic state, but generates seemingly random patterns with small-scale structures. (IV) It shows a mixture of order and randomness with long characteristic times. One class IV CA, rule 110, has been shown to emulate a universal Turing machine [19]. Shortcomings of this classification have been pointed out repeatedly, and other schemes have been proposed [20, 21, 22]. Also, it can happen that slow dynamics (which would put a CA into class IV) are hidden [23, 24], leading to misclassifications.

For a binary 1-d CA of lattice size L , there exist $N = 2^L$ different states $\mathbf{s}^{(a)} = (s_1^{(a)} \dots s_L^{(a)}), i = 0 \dots N-1$.

They form the nodes of a directed network with adjacency matrix \mathbf{A} , where $A_{ab} = 1$ if state a is mapped by the time evolution onto state b , i.e. $\mathbf{s}^{(a)}$ is a preimage of $\mathbf{s}^{(b)}$, and zero otherwise. This network typically consists of disconnected clusters, each containing a transient and a recurrent part. The latter forms an ‘attractor’, the entire cluster is its basin of attraction. Garden of Eden (GoE) states are transient states with zero in-degree. Pictures of some state space networks are shown in Fig. 1; for more see [8].

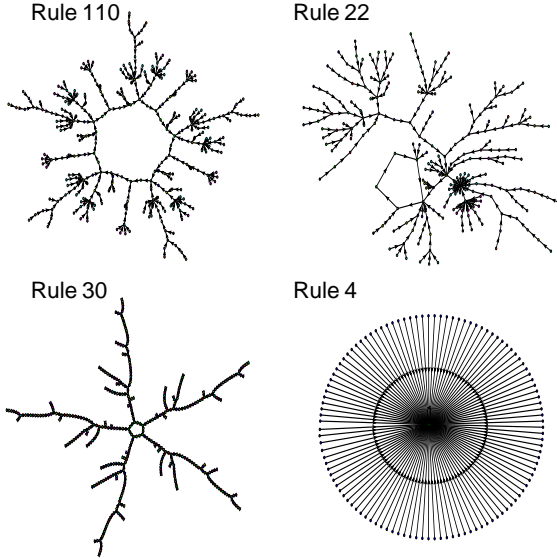


FIG. 1: Connected components of state space networks for different CA, plotted with program ‘Pajek’ (<http://vlado.fmf.uni-lj.si/pub/networks/pajek/default.htm>). All arrows are from leaves towards the center. Sizes are $L = 10$ to 13.

Since all nodes have unit out-degree, it is convenient numerically to replace A by the mapping list M : $M_a = b$, iff $A_{ab} = 1$. All network properties are computed from M straightforwardly. The attractor, in particular, is obtained by recursively removing nodes with zero in-degree, i.e. by constructing the ‘core’ with indegree = 1 (cf. the construction of k -cores of undirected graphs [25]).

Fig. 2 demonstrates our first numerical result: Several CA exhibit clean scaling for the in-degree of the largest hub, $k_{max} \sim N^\nu$, which sets in already for rather small lattices. Furthermore, the same scaling holds for the second, third, etc., largest hub (data not shown).

This scaling, including the value of ν , can be derived exactly, provided we know the structure of the hub state \mathcal{H} . The latter can be guessed easily for all CA shown in Fig. 2, while it is less obvious for others.

For rule 18, e.g., one finds numerically that $\mathcal{H} = (00 \cdots 00)$ for all L . The evolution rule for CA 18 is $001 \rightarrow 1, 100 \rightarrow 1$, and $s_1s_2s_3 \rightarrow 0$ for all other triples. Thus all sequences that do not contain 001 or 100 as substrings are preimages of \mathcal{H} . To count the number of these preimages, we use a transfer matrix method.

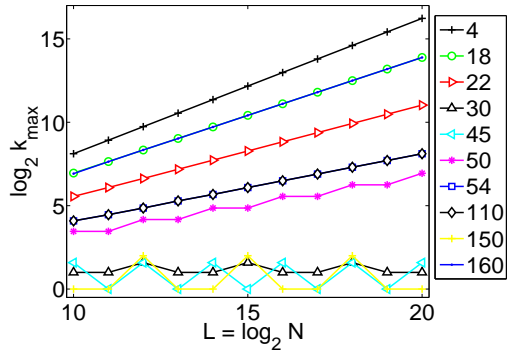


FIG. 2: The largest in-degree k_{max} as a function of $N = 2^L$. Except for class-III rules 30, 45 and 150, all CA show clear scaling of the largest hub size k_{max} with the total number of nodes in the network, N . Rule 160 is class I, 4 and 50 are class II, and 110 is class IV. Rules 18, 22, and 54 are between III and IV, as they have large structures masked by small-scale chaos (18, 22) or structures on intermediate scales (54).

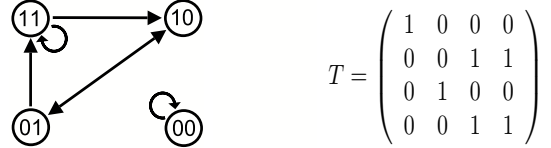


FIG. 3: Walks on the graph shown on the left generate all preimages of the hub state \mathcal{H} for rule 18. Each step corresponds to an element of the matrix T shown on the right.

The number of distinct strings of length ℓ without ‘001’ or ‘100’ is equal to the number of walks with $\ell - 2$ steps on the graph shown in Fig. 3. The number of periodic strings of length L is then given by $tr \mathbf{T}^L \approx N^{\log_2 \lambda_1}$, where \mathbf{T} is the matrix shown on the right of Fig. 3, and λ_1 is its largest eigenvalue. Notice that the basis vectors on which \mathbf{T} acts are the pairs 00, 01, 10, and 11 of neighbouring “spin” values. This gives $k_{max} \sim N^\nu$ with $\nu = \log_2 \lambda_1 = 0.6942$, in perfect agreement with the numerical results. Similar arguments hold for all CA that exhibited scaling in Fig. 2. A detailed comparison between numerical results and the predicted power laws is shown in Fig. 4.

A data collapse for the in-degree distribution function $P(k)$ for different system sizes is shown in Fig. 5 for rules 4, 22, and 110. For the range of L studied, these CA exhibit better collapse when using a multiscaling ansatz [26], as shown, rather than finite size scaling, which assumes power law behavior. Power laws would correspond to straight lines in Fig. 5 – whereas many distributions appear to be curving. To decide whether the apparent curvature is a finite size effect or a true indication of multiscaling is in general not easy, but it can be done analytically for rule 4. As Fig. 1 indicates, even though rule 4 has a broad in-degree distribution, it does not exhibit

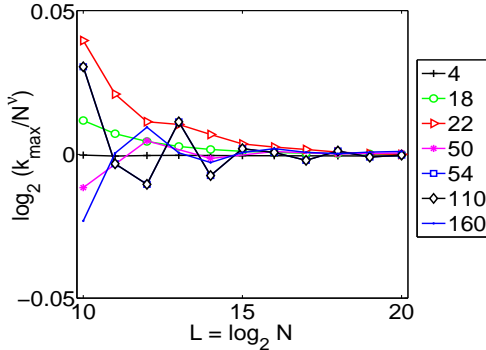


FIG. 4: Comparison between analytic and numerical simulation results. The analytic values of ν are 0.8114, 0.6942, 0.5515, 0.4057, 0.3471, 0.4057 and 0.6942 for rules 4, 18, 22, 50, 54, 110 and 160.

heterogeneity beyond the level of a single node.

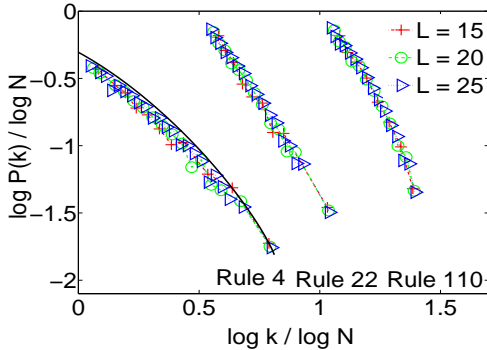


FIG. 5: In-degree distribution functions collapsed using a multiscaling ansatz for rules 4, 22, and 110 for different system sizes. The black solid line is the plot of Eq. (8). The distributions were shifted by 0.5 units each for clarity. Rule 22 is consistent with a power law $P(k) \sim k^{-\gamma}$ with $\gamma \approx 2.8$.

Since each node has out-degree one, the average in-degree must also be one. Nodes with high in-degree must therefore co-occur with many GoE states. The most common reason for the latter are finite forbidden sequences (FFS), i.e. finite sequences that have no preimage. Since almost every randomly chosen state of a large system will contain a FFS, most will be GoE states. When a FFS exists, states can be represented as a set of instances of the forbidden sequence with allowed subsequences filling the gaps between them. For certain rules this allows the in-degree distribution to be calculated.

For rule 4, the sequence $\dots 11 \dots$ has no preimage and the sequence $\dots 1 \dots$ has the unique preimage $\dots 010 \dots$. Consider a state that includes the sequence

$$\mathbf{s}_m = 01 0^m 10, \quad (1)$$

where 0^m is a string of m consecutive 0s. The preimages of \mathbf{s}_m are of the form

$$\mathbf{p}_m = 010 x^{m-2} 010, \quad (2)$$

where “ x^{m-2} ” represents any string of $m-2$ digits that does not contain the subsequence 010; i.e., any string that does not produce a 1 under Rule 4.

The number of strings of the form \mathbf{p}_m can be estimated using the same transfer matrix technique. The matrix

$$\mathbf{T} = \begin{pmatrix} 1 & 1 & 0 & 0 \\ 0 & 0 & 0 & 1 \\ 1 & 1 & 0 & 0 \\ 0 & 0 & 1 & 1 \end{pmatrix} \quad (3)$$

again is constructed such that it maps pairs $(s_{i-1}s_i)$ onto $(s_i s_{i+1})$, provided the output under the considered rule (i.e. rule 4) is $s'_i = 0$. To count all valid sequences, we must begin with $\mathbf{e}_3 = (0010)$ (standing for the pair $(p_2 p_3) = (10)$), apply \mathbf{T} m times from the right, and multiply finally with $\mathbf{e}_2 = (0100)$ which stands for $(p_{m+2} p_{m+3}) = (01)$. The number of ways to construct \mathbf{p}_m is thus

$$w_m = \mathbf{e}_3 \mathbf{T}^m \mathbf{e}_2^\top. \quad (4)$$

For large m we have $w_m \approx a \lambda^m$, where $\lambda = 1.75488\dots$ is the largest eigenvalue of \mathbf{T} and $a = 0.234487\dots = (\mathbf{e}_2 \cdot \mathbf{u})(\mathbf{v} \cdot \mathbf{e}_3)$, where \mathbf{u} and \mathbf{v} are the right and left eigenvectors corresponding to λ , normalized to $(\mathbf{v} \cdot \mathbf{u}) = 1$. This approximation becomes more accurate with increasing m . Any state containing n 1s will have an in-degree $k_n \approx \prod_{i=1}^n a \lambda^{m_i} = a^n \lambda^{L-n}$. Although occurrences of small m cannot be neglected, we find empirically that compensating errors make this formula reasonably accurate for large L . To find $P(k)$, all that remains is to count the states $\Omega(n)$ with n isolated 1s and no pairs ‘11’, and to transform the dependence on n into a dependence on k .

On a periodic lattice of length L , one has $\Omega(n) = C(L-n, n) + C(L-n-1, n-1)$, where $C(\ell, m) = \ell!/[m!(\ell-m)!]$. To obtain an approximation for $P(k)$ we first invert the above relation between k_n and n , giving

$$n(k) = \frac{L \ln \lambda - \ln k}{\ln(\lambda/a)}, \quad (5)$$

and then use $P(k) \approx 2^{-L} \Omega(n) |dn/dk|$.

The scaling ansatz shown in Fig. 5 is indeed recovered by this approximation. To see this, we define

$$x \equiv \ln k / \ln N, \quad y \equiv \ln P(k) / \ln N. \quad (6)$$

Then, Eq. (5) can be written as

$$\frac{n}{L} = \frac{\ln \lambda - x \ln 2}{\ln(\lambda/a)} \quad (7)$$

and $y \approx -1 - x + \ln[\Omega(n)]/(L \ln 2)$, where we have neglected a term $\ln \ln(\lambda/a)/(L \ln 2)$.

Using Stirling’s formula, we take the large L limit of $\ln[\Omega(n)]/L$ for fixed x and get

$$y \approx -1 - x + \log_2 \left[\frac{(1-\epsilon)^{1-\epsilon}}{\epsilon^\epsilon (1-2\epsilon)^{1-2\epsilon}} \right], \quad (8)$$

where $\epsilon \equiv n/L$ which is a function of x through Eq. (7). Eq.(8) is shown as a solid line in Fig. 5. The curvature of this line clearly indicates that there is no substantial range over which the distribution is a power law. Using a Fourier method based on recursion relations, we have also determined numerically the exact distribution for $L = 10,000$. For large x it is in excellent agreement with the above approximation.

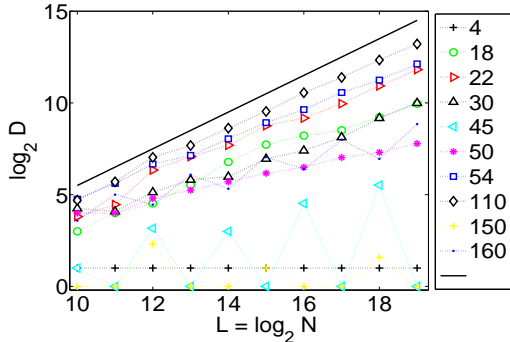


FIG. 6: The path diversity, \mathcal{D} of different CA. Straight lines indicate scaling behavior $\mathcal{D} \sim N^\delta$. Values of δ obtained numerically are 0.78, 0.87, 0.44, 0.81 and 0.94 for rules 18, 22, 50, 54 and 110 respectively. The straight line is a guide for the eye and has a slope of 1.

As Fig. 1 indicates, even though rule 4 has a broad in-degree distribution, it does not exhibit heterogeneity beyond the level of a single node. In order to distinguish the networks further we introduce a new quantity, the *path diversity* \mathcal{D} (see [3, 4] for similar measures). This is a measure of fluctuations in the paths from GoE states to attractors. First, we define a path diversity for each transient node: A GoE state has diversity one; a transient state with a single preimage has the same diversity as its preimage; and the diversity of a node with more than one incoming link is the sum of all *distinct* diversities of its preimages plus one. Thus, if a node has e.g. in-degree 5, and three of its preimages have diversity 2, one

has diversity 6, and the last has diversity 17, then that node's diversity is $(26 = 1 + 2 + 6 + 17)$. Finally, the path diversity \mathcal{D} of the entire CA is computed by joining all attractor states (in all disconnected components, if there are several ones) into one single “meta-state”, and applying the above scheme to the meta-state.

In Fig. 6, \mathcal{D} is shown for several CA rules. It clearly separates rule 4 (where $\mathcal{D} = 2$ for all L) as a low diversity system from other CA. Actually, other rules exhibit scaling behavior, $\mathcal{D} \sim N^\delta$ with $\delta = 0.78, 0.87, 0.44, 0.81$ and 0.94 for rules 18, 22, 50, 54 and 110 respectively. The CA's exhibiting strong fluctuations both globally and locally, i.e. having non-zero values for both ν and δ , include rules 18, 22, 50, 54 and 110. We do not presently have any analytic methods to determine values of δ , so it is possible that the observed values may be only approximate, and scaling may change at large sizes. This is particularly true for rules 18 and 50, which show already in Fig. 6 some deviations from perfect scaling. A striking feature of Fig. 6 are the large oscillations for rule 45. They arise because rule 45 on lattices with even L has no transients and only simple loop attractors, while the state space network is much less trivial for odd L . They highlight the subtle effects of global constraints.

In summary, we have studied networks formed by states of elementary 1-d CA on finite lattices. We have seen that some of them exhibit non-trivial scaling, and that this scaling can be computed analytically in many cases. The statistics of in-degrees (a local property) does not allow to distinguish between “simple” (Wolfram classes I and II) and complex (class IV) networks. But including the path diversity, which depends on the global structure of the network, allowed to make this distinction – subject to all the uncertainties related to Wolfram's classification, although (see rules 30 and 160) the diversity alone would not be sufficient for this either.

Part of this work was done at Perimeter Institute for Theoretical Physics. J.E.S.S and B.S. were supported by the NSF Grant PHY-0417372 and the Institute for Bio-complexity and Informatics at the University of Calgary. W.N. was supported by NSF Grant CHE-0313618.

[1] J. von Neuman, *Theory of Self-Reproducing Automata* (Univ. of Illinois Press, 1966).
[2] P. Grassberger, Int. J. Theor. Phys. **25**, 907 (1986).
[3] B.A. Huberman and T. Hogg, Physica D **22**, 376 (1986).
[4] C.P. Bachas *et al.*, Phys. Rev. Lett. **57**, 1965 (1986).
[5] R. Badii and A. Politi, Phys. Rev. Lett. **78**, 444 (1997).
[6] W. Bialek *et al.*, Physica A **302**, 89 (2001).
[7] D.P. Feldman *et al.*, Phys. Lett. A **238**, 244 (1998).
[8] A. Wuensche and M. Lesser, *The Global Dynamics of Cellular Automata* (Addision-Wesley, 1992).
[9] M. Baiesi *et al.*, Phys. Rev. E **69**, 066106 (2004).
[10] A. Barabasi *et al.*, Nature Rev. Genet. **5**, 101 (2004).
[11] A. Barabasi *et al.*, Physica A **281**, 69 (2000).
[12] M.E.J. Newman, Proc. Natl. Acad. Sci **98**, 404 (2001).
[13] M.E.J. Newman, SIAM Rev. **45**, 167 (2003).
[14] R. Albert *et al.*, Rev. Mod. Phys. **74**, 47 (2002).
[15] R. Albert, J. Cell Sci. **118**, 4947 (2005).
[16] D. Balcan and A. Erzan, Eur. Phys. J. B **38**, 253 (2004).
[17] S. Wolfram, *New Kind of Science* (Wolfram Media, 2002).
[18] S. Wolfram, Physica D **10**, 1 (1984).
[19] M. Cook, Complex Syst. **15**, 1 (2004).
[20] K. Cullik II *et al.*, Physica D **45**, 357 (1990).
[21] H.A. Gutowicz, Physica D **45**, 136 (1990).
[22] A. Dhar *et al.*, Phys. Rev. E **51**, 3032 (1995).
[23] P. Grassberger, Phys. Rev. A **28**, 3666 (1983).
[24] P. Grassberger, J. Stat. Phys. **45**, 27 (1986).
[25] S.B. Seidman, Social Networks **5**, 269 (1983).
[26] S. Lise and M. Paczuski, Phys. Rev. E **63**, 036111 (2001).